Electronic Supplementary Material (ESI) for Journal of Materials Chemistry B.

Supporting Information

Hang Xu [b,c], Xiuzhu Xu[a,d], Jiawei Xu[a,d], Shengping Dai[c], Xu Dong[c], Feng Han*[b], Ningyi Yuan*[c] and Jianning Ding *[a,c,d].

a. Institute of Intelligent flexible Mechatronics，Jiangsu University, Zhenjiang, 212013, China.

b. School of Pharmacy, Nanjing Medical University, Nanjing, 211100, China.

c. Jiangsu Collaborative Innovation Centre of Photovoltaic Science and Engineering, Jiangsu Province Cultivation Base for State Key Laboratory of Photovoltaic Science and Technology, Jiangsu Key Laboratory for Solar Cell Materials and Technology, Changzhou University, Changzhou, 213164, China.

d. Micro/Nano Science and Technology Centre, Jiangsu University, Zhenjiang, 212013, China.

*Email: dingjn@ujs.edu.cn; nyyuan@cczu.edu.cn

SEM imaging of the cross-section view.

The PDMS-CNT/Chitosan film was cut and the cross-section was captured on a field emission scanning electron microscopy (FESEM, Hitachi S-4800).

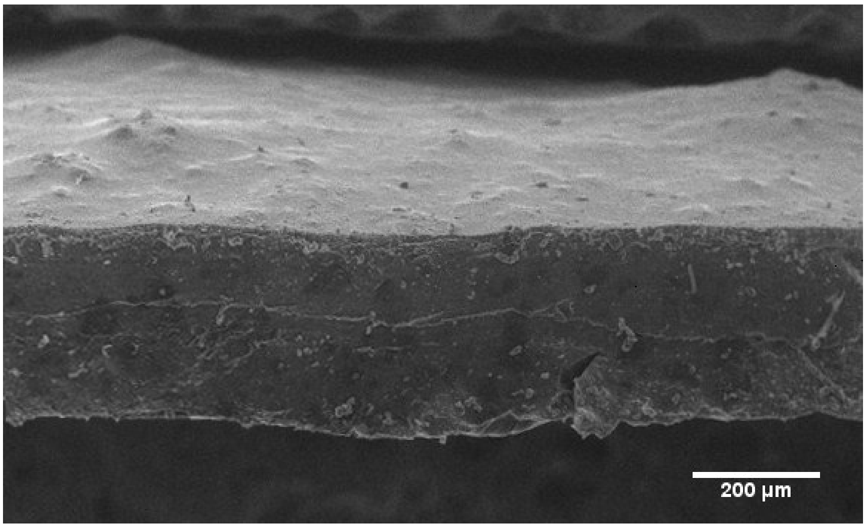

Figure S1 SEM image of the PDMS-CNT/Chitosan film's cross section.

Actuation behavior of the thicker PDMS-CNT/Chitosan film (thickness: 513.1um) under the irradiation of 500mW/cm^2 808nm light.

A PDMS-CNT/Chitosan membrane with higher thickness of 513.1um was fabricated and tested with a 500mW/cm^2 808nm near-infrared light irradiation.

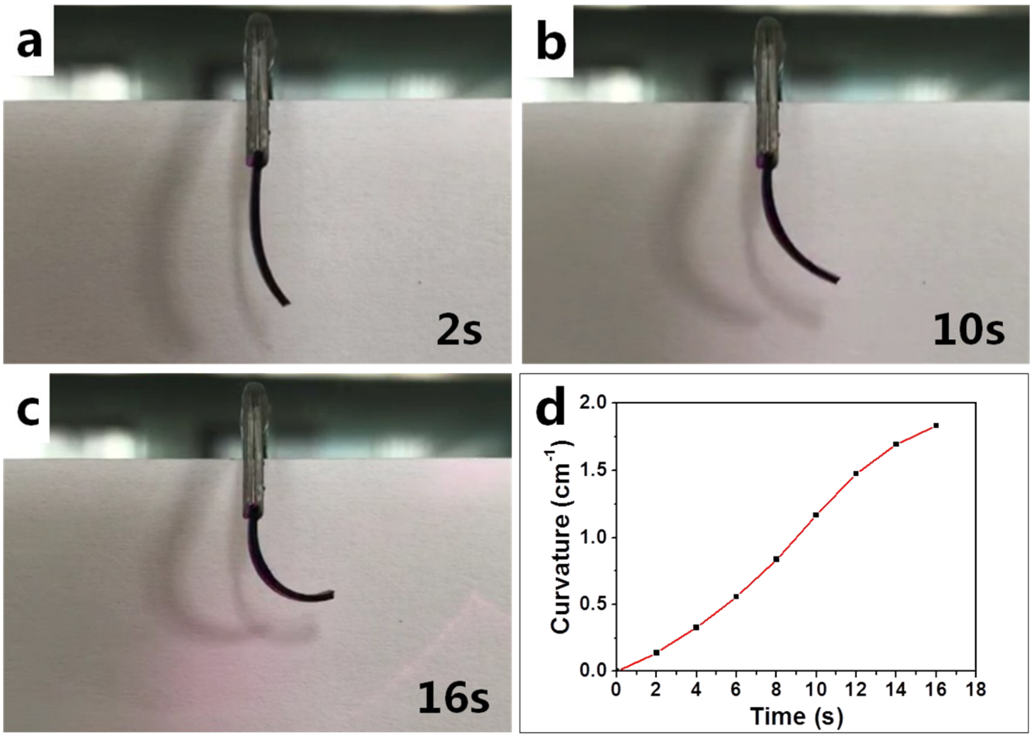

Figure S2 The actuation behavior of the PDMS-CNT/Chitosan membrane (thickness: 513.1um) under 500mW/cm^2 808nm light irradiation for 2s **(a)**, 10s **(b)**, 16s **(c)**, and Curvature-Time curve **(d)**.

The method of measuring and calculating the bending curvature.

The bending angle was measured as the **Figure S3** shows. Due to the significant influence of gravity and the uneven heat flux caused by the continuously changed heating surface with time, the shape of the dual layer film cannot be simplified into a circle. Thus, a tangent line was drawn to figure out the angle (a) to the y axis. Specifically, four conditions were considered: Condition A (a<π/2), B(π/2≤a<π), C(π≤a<3π/2), D(3π/2≤a<2π), corresponding to **Figure S3a-d**. The curvature was calculated as the following equation:

$$\text{Curvature} = \frac{Bending\ Angle\ (radian)}{Length\ of\ the\ Actuator}$$

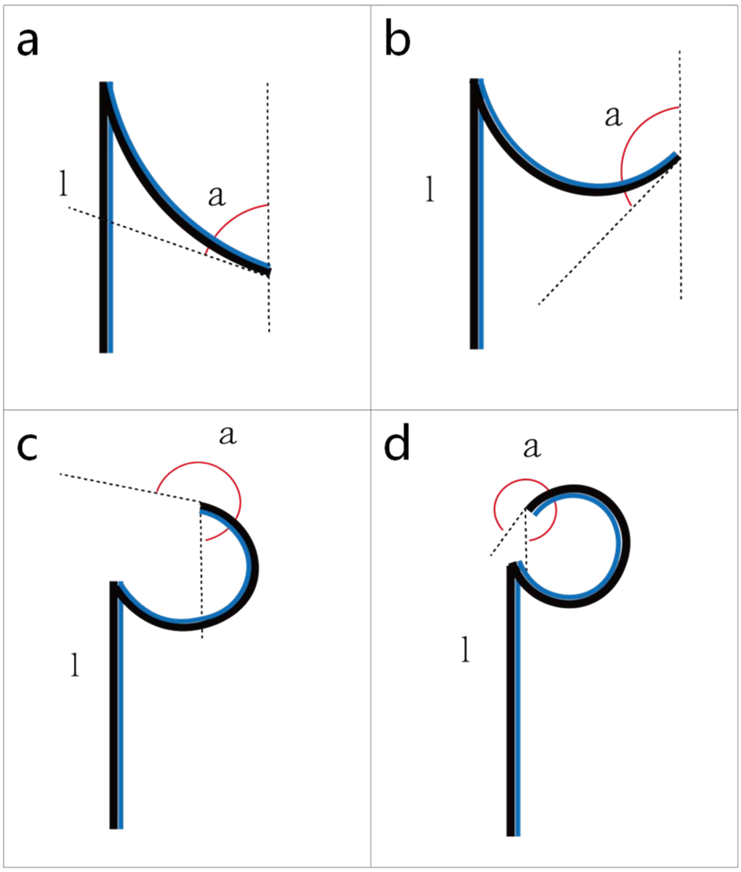

Figure S3 The Schematic diagram of the bending curvature measurement.

The measurement of the elastic modulus and the elongation at break.

The PDMS-CNT/Chitosan samples with different CNT contents (0%, 1%, 5%, 15%) were prepared for a tensile test on a universal testing machine (QT-6203S, Qian Tong Instrument Equipment Co. Ltd., Jiangsu) at a constant strain rate of 10 mm/min. The outcomes were listed in the **Table S1**. The curve of tensile force versus elongation for the one with 1% CNT was displayed in **Figure S4**.

CNT%	Elastic Modulus(kPa)	Elongation at break(%)
0	2017.87	119.424
1	2595.67	71.711
5	5826.58	50.175
15	9466.76	28.014

Table S1 Elastic modulus and elongation at break for the PDMS-CNT/Chitosan samples with different CNT contents.

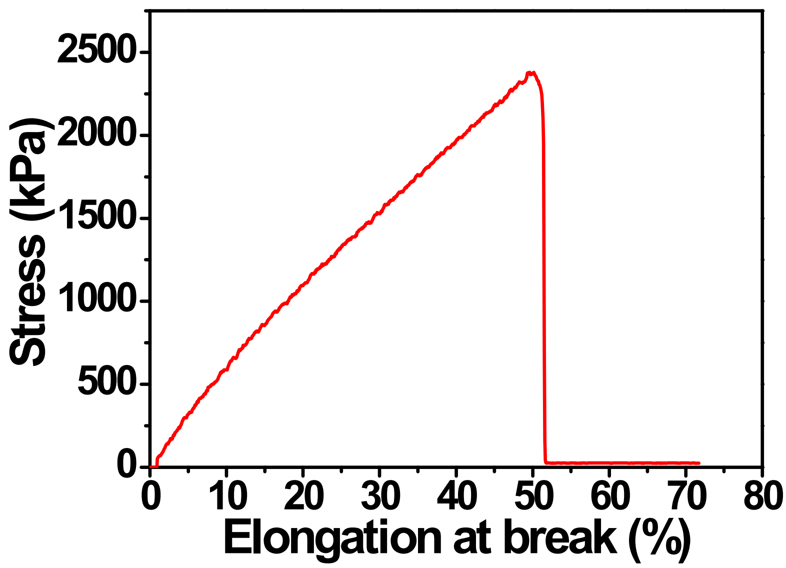

Figure S4 The tensile force versus elongation for the PDMS-CNT/Chitosan samples with 1% CNT.

Element finite analysis of the PDMS-CNT/Chitosan film's mechanics.

The mechanic modeling was performed on a COMSOL® Software Version 5.4 by a finite element analysis.

1. Physics model

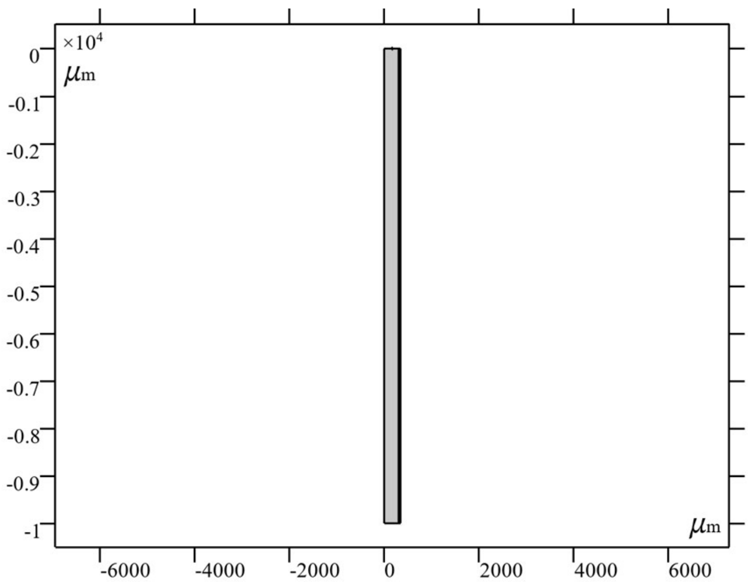

In this model , the bilayer membrane's length is 1cm, the bilayer membrane's width is 0.135cm, the thickness of PDMS is 301.9um, and the thickness of chitosan film is 41.1um.

2. Control functions

2.1. Solid Mechanics

$$\rho\frac{\partial^2 \mathbf{u}}{\partial t^2} = \nabla \cdot \mathrm{S} + \mathbf{F}_\mathrm{V}$$

$$\mathrm{S} = \mathrm{S}_{\mathrm{ad}} + \mathbf{C} : \epsilon_{\mathrm{el}} - \frac{1}{3}(\epsilon_{\mathrm{vol}} - \epsilon_{\mathrm{w}})\mathbf{C} : \mathrm{I}, \quad \epsilon_{\mathrm{el}} = \epsilon - \epsilon_{\mathrm{inel}}$$

$$\epsilon = \frac{1}{2}\left[(\nabla \mathbf{u})^{\mathrm{T}} + \nabla \mathbf{u}\right]$$

$$\mathbf{C} = \mathbf{C}(E, \nu)$$

u is the displacement vector, $\mathbf{F}_v$ is the volume force vector, **S** is the second Piola-Kirchhoff stress. **C** is the 4th order elasticity tensor, and E, v represents Young's modulus and Poisson's ratio, respectively. ':' stands for the double-dot tensor product. The elastic strain ε_{el} is the difference between the total strain ε and all inelastic strains ε_{inel}. The ε_{vol} and ε_w is the volume strain and the strain along w axis. S_{ad} is defined as the energy variation.

2.2. Solid Heat transfer

$$\rho C_p \frac{\partial T}{\partial t} + \rho C_p u \cdot \nabla T + k_p \nabla^2 T = Q$$

2.3. Deformed Geometry

$$x_n = \int_{xn} \alpha_n(T_{s,n}(t) - T_{ref,n})dx_n$$

$$y_n = \int_{yn} \alpha_n(T_{s,n}(t) - T_{ref,n})dy_n$$

Where x_n, y_n is the total displacement of x and y axis. a_n is deformed as thermal expansion coefficient of each material.

3. Boundary conditions

3.1. Solid Mechanics

3.1.1 Fixed constraint boundary

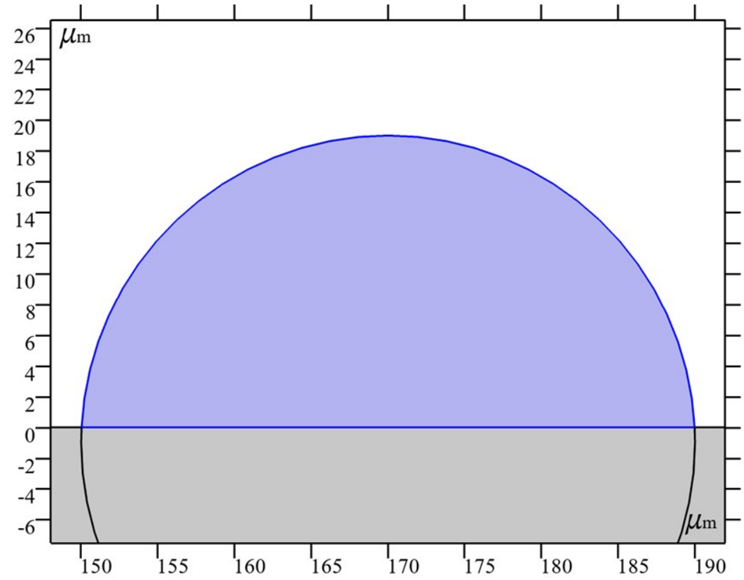

The fixed constraint boundary is on the top of the physics model.

3.1.2 Free deformation

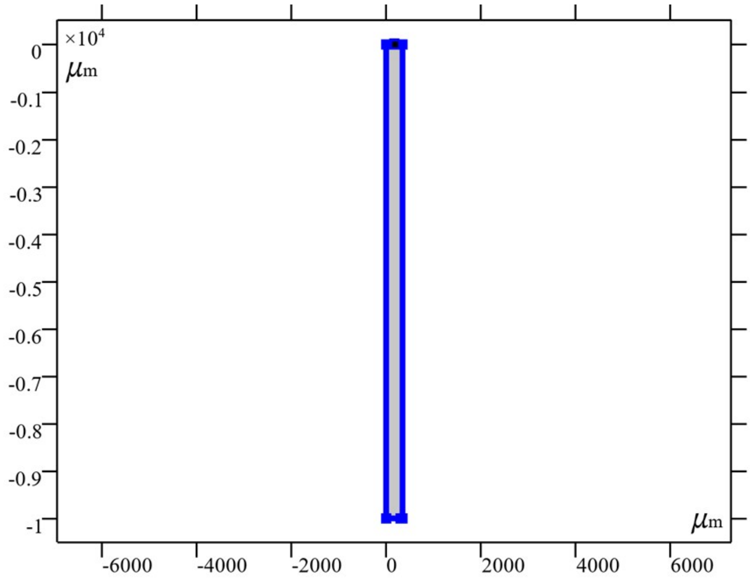

3.1.3 Body force

In this model, body force is only deformed with the gravity.

3.2 Solid Heat transfer

3.2.1. Fixed temperature boundary

The position of the physic model, clamped by a tweezer, is defined as the fixed temperature boundary because the temperature in this area didn't change obviously in whole experiment.

3.2.2. Heat Flux

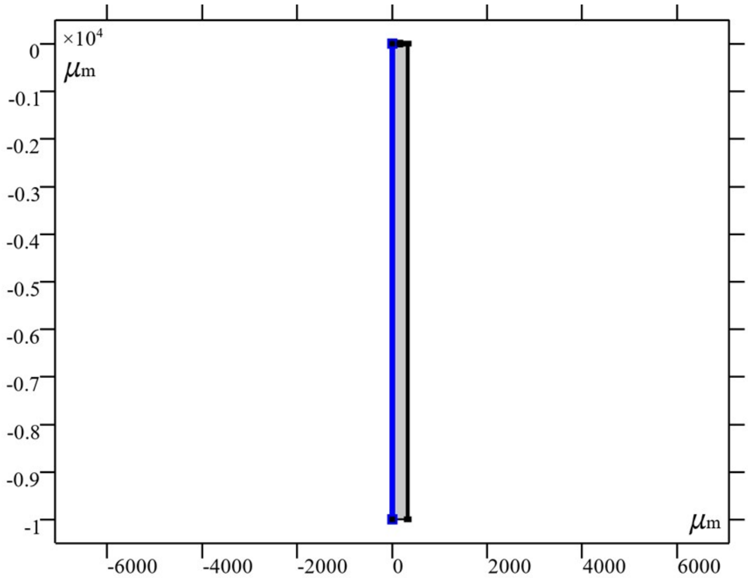

In the experiment, we used infrared light to heat the film, and the power is controlled from 100 to 500 mW/cm^2 with 100 mW/cm^2 interval. As the PDMS film considered as a graybody, we defined the absorbance of PDMS as 0.85. So the heat flux q_0 is 0.85*w_b, where w_b is the power of the infrared light. Obviously, the heat flux of the infrared light is an important parameter that influences the shape change of the film. In another model, the physics model is segmented into two parts, where the heat flux is fixed as 0.85*w_b in the upside part and -(0.85*w_b/169)*(t-3)^2+0.85*w_b in another part.

3.2.3 Heat extraction boundary condition

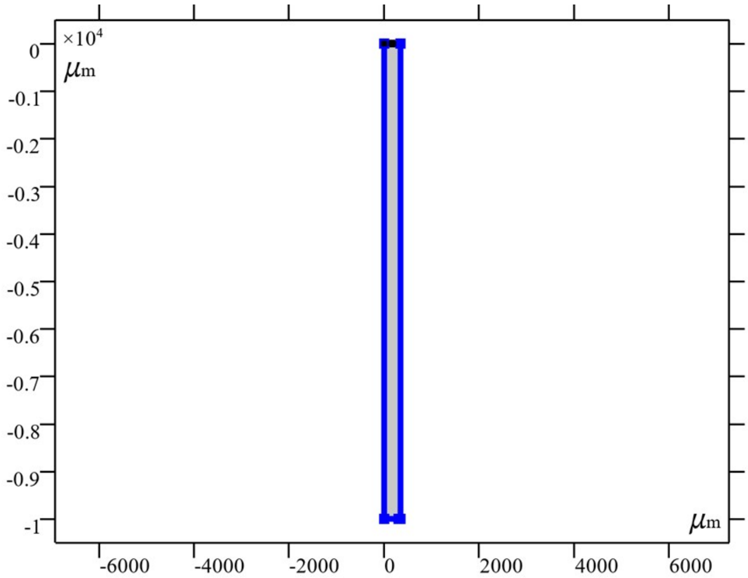

The heat extraction on the bottom of film can be defined as a free convection boundary,

$q_1 = \mathrm{h} \cdot (T_{out} - T(t))$

Where q_1 is the extraction on the film bottom, h is the convection heat transfer coefficient and T_{out} is the environment temperature which is 293.15K here. In our experiment, the environment is set as a windless space that the coefficient h can be defined as

$\frac{K_{air}}{L} 0.27 Ra_L^{\frac{1}{4}}$, *where L is the length of the mathatic model.*

3.2.4. Dynamic mesh

All material space and boundary is free.

4. Parameter Table

Name	Value	Description
roh1	1395 kg/m³	Chitosan density
aph1	-1.1E-3 1/K	Chitosan thermal expansion coefficient
k1	0.2 W/(m·K)	Chitosan heat conductivity
v1	0.3	Chitosan poisson ratio
E1	5.39E6 Pa	Chitosan Young modulus
C1	1900 J/(kg·K)	Chitosan specific heat capacity
roh2	970 kg/m³	PDMS density
aph2	3.1E-4 1/K	PDMS thermal expansion coefficient

k2	0.195 W/(m·K)	PDMS heat conductivity
v2	0.46	PDMS posisson ration
E2	2.6E6 Pa	PDMS Young modulus
C2	1575.4 J/(kg·K)	PDMS specific heat capacity
W_b	3535 W/m²	Illumination intensity
E_flux	0.85	Illumination absorptivity

Roh1, E1, v1 was obtained from the reference 1. Aph1 was obtained from the reference 2. E2 was obtained from our measurement. V2 was obtained from the reference 3. Roh2, k2, C2 were obtained from the reference 4. Aph2 was obtained from the reference 5. W_b was obtained by dividing 5000 W/m2 with $\sqrt{2}$, due to the 45°C of the light incidence to the surface of the membrane.

Reference

1. C.K. Sterzer, D.R. Sanchez, C.K. Rha, Makromol Chem, 1982, **183**, 1353-1359.
2. P.A. Do, M. Touaibia, A. Hache, Applied Optics, 2013, **52(24)**, 5979-5984.
3. B. Sarrazin, R. Brossard, P. Guenoun, F. Malloggi, Soft Matter, 2016, **12**, 2200-2207.
4. J Hong, H.S. Choi, K.S. Lee, S.E. Shim, Polymer International, 2012, **61(4)**, 639-645.
5. W.T. Wes, F. Shirin, J.H. Sangyoon, W. Junlan, J.S. Nathan, Journal of Micromechanics and Microengineering, 2011, **21(5)**, 54013-9.